TIME DOMAIN VELOCITY SELECTION MODULATION AS A TOOL TO EVALUATE CESIUM BEAM TUBES

Helmut Hellwig, Stephen Jarvis, Jr., D. J. Glaze
Donald Halford, and Howard E. Bell

Time and Frequency Division
National Bureau of Standards
Boulder Colorado 80302
Tel.: (303) 499-1000 Ext. 3207

Summary

Pulsed excitation of atomic and molecular beam devices with separated Ramsey-type interaction regions allows the observation of signals due to very narrow atomic velocity groups. The theoretical background of this method is discussed. Experimental operation of a near mono-velocity cesium beam tube is demonstrated. The velocity distribution of a commercial cesium beam tube and of the primary laboratory standard NBS-5 are obtained using the pulse method. The normal Ramsey patterns are calculated from the velocity distribution and compared with the measured Ramsey patterns. The pulse method allows the direct determination of the cavity phase shift and of the second-order Doppler correction in beam devices. Velocity distributions obtained via the pulse method allow the use of microwave power shift results for accuracy evaluations. These aspects as well as the effects of modulation and different velocity distributions are discussed in detail. The pulse method thus shows promise for the evaluation of existing laboratory as well as commercial cesium beam tubes with respect to these effects.

Key words. Atomic beams, Cavity phase shift, Cesium beam, Frequency standard, Pulsed excitation, Second-order Doppler shift, Velocity distribution.

Introduction

In the course of the accuracy evaluation of primary laboratory cesium beam standards, it has become important to know precisely the velocity distribution of the atoms which interact with the microwave field [1-3]. Once the velocity distribution is known, it is possible to calculate the second-order Doppler shift correction for the particular device. It is also possible to determine the cavity phase shift [2, 4, 5] from additional experimental knowledge such as frequency shifts of the resonance frequency with beam reversal, with velocity, with the exciting microwave power, and with the modulation deviation*. In addition, the knowledge of the velocity distribution may be expected to give considerable insight into the performance of the beam optics and thus may allow diagnostic testing of the beam tube and its optical system.

The velocity distribution cannot be simply inferred from the oven temperature because the beam optics will modify the distribution to a significant extent. We were therefore searching for measurement methods which would allow the direct determination of the velocity distribution in the microwave cavity. The separated oscillatory field method as introduced by Ramsey[6], is almost universally used in both commercial and laboratory cesium beam standards. The atomic beam passes sequentially through the two cavity sections. Thus, the Ramsey-type cavity offers itself in a natural way as a means to determine velocity distributions using the time of flight principle.

In conventional cesium beam designs, the two separated interaction regions are part of the same cavity. It is therefore impossible to operate the two cavity sections independently in order to achieve a probing of the atomic velocities. In the following we will show that pulses applied to the cavity as a whole, allow selectivity towards certain velocities.

Theoretical Considerations

Let us consider the interaction between the atomic beam and a pulsed microwave field in the cavity. Most atoms will not be subjected to any microwave interaction because only a few atoms will be in the cavity interaction regions when the pulses occur. Those atoms which do experience a pulse in only one of the two separated cavity sections will undergo transitions with certain transition probabilities. The corresponding frequency dependence will be given by the interaction time of the atoms with the pulsed microwave field. The linewidth in the frequency domain will therefore be approximately equal to the inverse interaction time. However, there will be groups of atoms which are able to interact successively with both fields in the two cavity sections. These are those atoms whose velocities v lead to a time of flight between the two cavity sections which is equal to the inverse pulse frequency T (time between pulses). With L being the distance between the two cavity sections we have for these preferred velocities:

$$v = \frac{L}{T} \qquad (1)$$

The frequency domain behavior of this velocity group is approximately given by the mono-velocity Ramsey pattern equation. Near resonance we therefore can use eq V 44a of [6] to describe the spectral behavior of the velocity group given by eq (1). We use Ramsey's notation.

$$\langle P \rangle = \sin^2 2b\tau \cos^2 \frac{1}{2}(\lambda T - \delta) \qquad (2)$$

where P is the transition probability. The microwave field parameter b is proportional to the square root of the microwave power. The frequency parameter λ is given by $\lambda \equiv \omega_0 - \omega$ where ω_0 is the atomic (angular) resonance frequency, ω is the (angular) driving frequency, and δ is the phase difference between the two microwave cavity sections; τ is the interaction

* A low frequency modulation of the existing microwave signal is used in the servo electronics to locate line center.

time of the atoms with the microwave field. Equation (2) allows us to discriminate between the signal due to transitions caused by the interaction in just one single cavity section in which the whole velocity distribution participates and the signal due to the successive interactions in both cavities, which is generated by a certain narrow velocity group. If we vary the frequency we find that the signal due to the single cavity interaction ($2\sin^2 b\tau$) essentially stays constant in the vicinity of the atomic resonance frequency. The Ramsey signal given by eq (2), however, varies strongly with λ.

Let us assume for the following that we keep the argument $2b\tau$ of the sine function constant. In this case, we can show that our Ramsey signals (amplitude of the Ramsey pattern) can be written as:

$$S \sim t_o \Delta v f_p \rho(v)\, r(f_p)\, P_{p,q} . \tag{3}$$

Here t_o is the on-time, i.e., the portion of one pulse period during which the detector receives atoms which have been subjected to successive interactions in both cavities. Δv is the velocity window, f_p is the pulse frequency, ρ is the velocity distribution function, and r is the system response including the detector response. The product $t_o f_p$ could be called the duty cycle of the beam tube. If we know all of the other parameters, we can calculate the velocity distribution ρ from a measurement of the amplitude of the Ramsey pattern, i.e., the difference between peak and valley of the Ramsey pattern. The pulse frequency obviously is given by

$$f_p = \frac{1}{T} . \tag{4}$$

and, from eq (1), we can write the velocity window

$$\Delta v = \frac{1}{T}\,\Delta L + \frac{L}{T^2}\,\Delta T , \tag{5}$$

where ΔL and ΔT represent the finite interaction length and interaction time of the atoms with the microwave field. In eq (6) we can substitute $\Delta L \approx \ell$ and $\Delta T \approx \tau_\rho$ and obtain in good approximation

$$\Delta v \approx \frac{\ell}{T} + \frac{L}{T^2}\,\tau_p , \tag{6}$$

where ℓ is the length of the single cavity region, and τ_ρ is the pulse duration.

We now consider short pulses, i.e., pulses with durations short compared to the time of flight through the single cavity or

$$\tau_p < \frac{\ell}{v} = \frac{\ell}{L}\,T . \tag{7}$$

The velocity window is then given by

$$\Delta v \approx \frac{\ell}{T} \tag{8}$$

and the on-time by the time which the atoms spend in the cavity or

$$t_o \approx \frac{\ell}{v} . \tag{9}$$

We note that the on-time is quite different from the interaction time of the individual atoms with the microwave field, which is now simply given by the pulse duration τ_p. We further note that the previously assumed $2b\tau \approx$ const is here automatically fulfilled, because b can easily be held constant while $\tau \equiv \tau_p$, and thus is given and set by the experimentalist. If we assume that we can keep the system response also constant, we obtain the velocity distribution as

$$\rho(v) = \text{const } ST. \tag{10}$$

The fact that $\tau \equiv \tau_p$ is interesting, because it means that all atoms experience the same transition probability regardless of their velocity which is quite in contrast to the usual cw operation of a beam tube. The measurement procedure for short pulses is then simply to sweep the frequency through at least one peak and one valley of the Ramsey pattern at each of a variety of pulse frequencies while keeping the pulse duration constant. The microwave power must also be kept constant. The resultant values have then to be multiplied with T in order to obtain the velocity distribution without further corrections.

Of course, signals will be contributed too from sub-multiples of the selected velocity (eq (1)). However, it is easy to discriminate between signals from different harmonically related velocities simply by their obvious harmonic relationship in the Ramsey pattern. For most beam tubes, we may expect to encounter at most the first sub-harmonic because of the typically fairly narrow velocity distributions. Atoms with velocities v = L/T will interact with every second pulse of the pulse-train if measured as the first sub-harmonic at the pulse frequency $f_p^1 = \frac{2}{T}$. The on-time and the velocity window at this higher frequency stay the same as when the atoms are measured at $f_p^o = \frac{1}{T}$. As compared to the corresponding signal of the same velocity group when observed as the fundamental signal at f_p^o, the measured signal at f_p^1 will double. This doubling can serve as an easy check for the adequacy of the system response at higher pulse frequencies.

We now consider the case of long pulses. In this case, the interaction time of the atoms with the field is given by their time of flight through the single cavity or

$$\tau_p > \frac{\ell}{v} = \frac{\ell}{L}\,T. \tag{11}$$

For this case, the velocity window reduces to

$$\Delta v \approx \frac{L}{T^2}\,\tau_p . \tag{12}$$

The on-time t_o of the beam tube is now given by the pulse duration τ_p. Using eq (3), we can therefore obtain the velocity distribution as

$$\rho(v) = \text{const } ST^3 \tau_p^{-2} . \tag{13}$$

If we keep the ratio τ_ρ/T constant, this equation

simplifies to

$$\rho(v) = \text{const } ST. \tag{14}$$

For eqs (13) and (14), we again assumed $2b\tau$ = const. For long pulses this condition is not as easily fulfilled as it was for short pulses. However, from the condition $2b\tau = \frac{\pi}{2}$ for optimum power we obtain with $\tau = \ell T/L$ and $b \sim \sqrt{P}$

$$\frac{P}{P_o} = \left(\frac{T_o}{T}\right)^2 \tag{15}$$

where P_o is optimum power for some given T_o, and P is optimum power for other pulse times T. We notice that we do not have to worry about the first sub-harmonic as an interferring signal because it will always be at a power setting which leads to $2b\tau = \pi$, and thus not contribute. If we adjust, however, the power to be optimum for some first sub-harmonic signal, then this signal will be exactly half of the corresponding signal of the same velocity group when observed as the fundamental signal. This follows from the fact that, under the condition of τ_p/T = constant, the pulse frequency doubles while the on-time and the velocity window are cut in half.

Since it appears prudent to choose a velocity window which is narrow enough to permit adequate resolution, but large enough to still give a reasonable signal to noise, it is obvious that the short-pulse method is the choice in the case of rather short beam tubes, whereas the long-pulse method is best applied for long laboratory type devices. The loss of atoms in pulsed operation as compared to cw operation is approximately given by $\Delta v/D \times t_o/T$, where D is the width of the velocity distribution. Thus, a velocity window of, e.g., 10 percent of the most probable velocity will lead to a signal of approximately one percent of the cw signal and a corresponding frequency stability loss of about one order of magnitude (if shot noise limited).

Application in Accuracy Evaluations

The pulse method allows a direct determination of the phase difference between the two cavity sections. From eq (2), we obtain the shift in the resonance frequency due to a cavity phase shift as

$$\Delta v = -\frac{\delta}{2\pi L} v . \tag{16}$$

It is now necessary to include the second-order Doppler shift into our considerations. Its combination with the cavity phase shift leads to a total velocity dependent bias of

$$\Delta\nu = -\frac{1}{2}\nu_o \frac{v^2}{c^2} - \frac{\delta}{2\pi L} v \tag{17}$$

where ν_o is the atomic resonance frequency, and c the speed of light.

From the change in the frequency shift $(\Delta\nu_1 - \Delta\nu_2)$ due to operation at two different velocities v_1 and v_2 (pulse separations T_1 and T_2) we obtain the phase shift δ as

$$\delta = -2\pi L\left\{\frac{1}{2}\nu_o \frac{v_1 + v_2}{c^2} + \frac{\Delta\nu_1 - \Delta\nu_2}{v_1 - v_2}\right\} \tag{18}$$

and the frequency bias $\Delta\nu$ for a particular velocity v is

$$\Delta\nu = \frac{1}{2}\nu_o \frac{v}{c^2}\left\{v_1 + v_2 - v\right\} + \frac{\Delta\nu_1 - \Delta\nu_2}{v_1 - v_2} v . \tag{19}$$

Obviously, eq (19) simplifies for special choices of v.

In pulsed operation the Ramsey pattern will be located on a Rabi-type pedestal which is given in the case of long pulses by the transit time ℓ/v of the atoms through the single cavity section. For the short pulses, however, this pedestal is given by the pulse length τ_p and can therefore be considerably wider than the pedestal obtained under cw operation. Therefore, in the case of short pulses, care must be taken to keep the Rabi pedestal somewhat narrower than the separation of the magnetic field dependent transitions; otherwise, the pulses will excite the magnetic field dependent transitions and cause erroneous results in the pulsed operation of the beam tube.

The velocity distribution, which can be obtained from the application of the pulse method, may be used to obtain quantitative data on cavity phase difference and second-order Doppler effect from frequency shift measurements with varying microwave interrogation power [2, 4, 5]. The microwave power which is fed into the interaction region selects certain velocities within the given velocity distribution. The effective velocity is therefore a function of the microwave power* and frequency shifts can be interpreted as due to changes in the effective velocity.

The relationships involved may be obtained quantitatively as follows: The mean transition probability close to resonance can be written as

$$\langle P\rangle = \int dv\, \rho(v) \sin^2 \frac{2b\ell}{v} \cos^2 \frac{\lambda' L}{2v} \tag{20}$$

where

* Frequency shifts may be associated with microwave spectrum impurities. Thus, extreme care is necessary in assuring a sufficiently clean microwave spectrum before interpreting power shifts as outlined above.

$$\frac{\lambda' L}{2v} = \frac{L}{2v}\left(\lambda + \frac{v^2}{2c^2}\,\omega_o\right) + \frac{\delta}{2}. \qquad (21)$$

If desired, a term for the modulation deviation can be included in eq (21).

At resonance, $\frac{dP}{d\lambda} = 0$, we obtain as the frequency bias

$$\lambda = - v_D^2 \frac{\omega_o}{2c^2} - v_P \frac{\delta}{L} \qquad (22)$$

with the effective velocities v_D and v_P given by:

$$v_D^2 = \frac{\left\langle \sin^2 \frac{2b\ell}{v} \right\rangle}{\left\langle \frac{1}{v^2} \sin^2 \frac{2b\ell}{v} \right\rangle} \qquad (23)$$

$$v_P = \frac{\left\langle \frac{1}{v} \sin^2 \frac{2b\ell}{v} \right\rangle}{\left\langle \frac{1}{v^2} \sin^2 \frac{2b\ell}{v} \right\rangle} \qquad (24)$$

using $\langle \cdots \rangle = \int dv\, \rho(v) \cdots$

For two different microwave power settings, high (H) and low (L), we can numerically calculate v_D and from eq (23) and (24). This requires that the velocity distribution $\rho(v)$ is known (e. g., from the pulse method) and that the field parameter b is known. The pulse method allows a determination of b through optimizing the signal at a certain pulse setting corresponding to a known velocity. This forces $\frac{2b\ell}{v} = \frac{\pi}{2}$ and-since ℓ is well known - permits determination of b. Alternately, b can be obtained from optimally matching the experimentally obtained Ramsey pattern to one calculated from the known $\rho(v)$ using b as the adjusting parameter.

The cavity phase difference can then be calculated as

$$\delta = - 2\pi L \left[\frac{\nu_o}{2c^2} \frac{v_{DH}^2 - v_{DL}^2}{v_{PH} - v_{PL}} + \frac{\nu_H - \nu_L}{v_{PH} - v_{PL}} \right] \qquad (25)$$

The frequency bias at some microwave power corresponding to the velocities v_{DO} and v_{PO} is then

$$\nu - \nu_o = - v_{DO}^2 \frac{1}{2} \frac{\nu_o}{c^2} - v_{PO} \frac{\delta}{2\pi L}. \qquad (26)$$

Experimental Results

For testing of the time domain velocity selection modulation (pulse method), we used a commercial cesium beam tube with an interaction length of L = 25 cm. The pulsing was done with an X-band pin-diode switch of about 80 dB attenuation and a few nano-seconds rise time. This allowed fast, clean switching with minimum transient effects. Fig. 1 depicts a microwave pulse of nearly 5 μs duration as measured directly at X-band with a sampling unit. Fig. 2 depicts the leading edge of the pulse in higher resolution. The power level could be adjusted with a precision attenuator. It should be noted here that for the pulse method -- in particular, the short-pulse method -- considerably higher powers are required than for normal cw operation. The signal was detected with either an electrometer or a synchronous detector, operated in synchronism with the pulse frequency. Both pulse frequency and pulse duration could be independently adjusted. The rise time of the pulse generator was compatible with the very fast switching time of the pin-diode. Fig. 3 shows the block diagram of the simple setup. The signal was obtained by either slowly sweeping through the Ramsey pattern or by measuring the difference between peak and valley of the Ramsey pattern using pre-calculated frequency settings. The sweep system consisted of an X-band klystron which was injection-locked to the signal output of a mixer in which the multiplied signal from a crystal oscillator at 9. 18 GHz was mixed with the signal of a frequency synthesizer. The frequency synthesizer was eigher adjusted manually or swept by remote programming.

In Fig. 4 the normal microwave spectrum of the beam tube is depicted with the magnetic field independent transition giving the biggest Ramsey pattern in the center of the figure. Fig. 5 shows, on the same horizontal scale with the same beam tube, the signal obtained with pulsed operation. The pulse duration was 45 microseconds; the pulse separation was T = 1. 8 ms corresponding to an atom velocity of 140 m/s. This velocity was identified as approximately the peak of the velocity distribution. The fractional velocity window is $\Delta v/v \approx \ell/L$ and thus about 4 percent. Accordingly, Fig. 5 shows a Ramsey pattern extending across the whole Rabi pedestal. The Rabi linewidth is wider than in Fig. 2 because the pulse duration for Fig. 5 is only 45 μs. If the pulse is further shortened to 15 μs, the Rabi line broadens by a factor of 3 as compared to the 45 μs pulse. As a result, the magnetic field dependent transitions totally overlap with the magnetic field independent transition, and we obtain a spectrum which is depicted in Fig. 6. An increase in the magnetic field would again separate this spectrum into the individual Rabi lines. It should be noted that the sweep time for Fig. 4 through 6 for the whole spectrum was about one hour.

Figures 7 and 8 show higher resolution traces of the Ramsey pattern. These figures serve to illustrate how the velocity distribution was obtained. Both were taken with pulse durations of 45 μs. In Fig. 7 the pulse separation was T = 1. 8 ms corresponding to a velocity of v = 140 m/s. In Fig. 8 we have T = 1. 2 ms corresponding to a velocity of about v = 210 m/s. Fig. 8 illustrates the separation of the wanted signal (v = 210 m/s) from the first sub-harmonic

velocity (v = 105 m/s). This sub-harmonic appears with twice the periodicity of the wanted signal in the Ramsey pattern and can thus easily be separated by harmonic analysis.

From the amplitude of a series of measurements like those depicted in Figs. 7 and 8 and from eq (10), we obtained the velocity distribution as shown in Fig. 9. The crosses depict measurements obtained from the pulse duration of 45 μs; the circles are values obtained with a pulse duration of 15 μs using an increased magnetic field in order to separate adequately the Rabi pedestals of the magnetic field dependent transitions. It is possible to calculate from this velocity distribution the normal Ramsey pattern of the beam tube (under cw operation). The calculation is numerical and computer-aided and follows eq V 37 of Ref. [6]. Fig. 10 shows a comparison of the calculated Ramsey pattern and the measured Ramsey pattern, both under optimum power conditions. The agreement is quite satisfactory considering that, from our experience, fairly small variations in the shape or placement of the velocity distribution will cause quite significant deviations of the calculated Ramsey pattern from the experimentally obtained Ramsey pattern.

We also are using successfully[7] the pulse method in the evaluation of our new primary frequency standard NBS-5. Because of the interaction length of nearly four meters for this device it is necessary to use the long pulse method. In Fig. 11 the velocity distribution of NBS-5 for an on-axis alignment is depicted and Fig. 12 gives a comparison between the Ramsey pattern which was calculated from Fig. 11 and the experimentally measured pattern. Using eq (23) and (24), the mean velocities v_D and v_P can be computed as a function of the microwave power. Fig. 13 depicts such calculation for the commercial tube (corresponding to Fig. 9) and Fig. 14 for NBS-5 (corresponding to Fig. 11). We note that v_D and v_P are somewhat different throughout, that the maximum obtainable change in mean velocity with microwave power is about 20 to 30% and that the mean velocity drops again (and oscillates) for higher microwave powers.

If we include the modulation term in eq (21) we are in a position to evaluate the mean velocity as a function of the modulation deviation. Figs. 15, 16, and 17 depict such plots for the commercial tube corresponding to the velocity distribution of Fig. 9, for NBS-5 corresponding to an off-axis alignment (distribution is Fig. 10 of Ref. [7]), and for a Maxwellian distribution with velocity cut-offs comparable to the NBS-5 system. In all three figures only v_P is plotted and several curves for different power parameters b are shown. All three figures show that regardless of the particular velocity distribution the mean velocity changes by not more than 5% if the modulation deviation does not exceed the half-linewidth and the microwave power is not excessively above optimum power. * A 5% change in the mean velocity results in a 5% change in the phase shift term and a 10% change in the second-order Doppler term (comp. eq (17)), and thus is usually negligible in the case of carefully built laboratory devices.

* These results confirm the conclusions of the simple treatment given in Ref. [4] and [5]; however, they are somewhat at variance with the results of Ref. [2].

Applications

A crystal oscillator can be servoed to the cesium beam tube while using time velocity selection modulation. For this a digital switching servo is desirable. Locking a crystal oscillator to essentially a mono-velocity beam and the ability to change that velocity within the range given by the velocity distribution in the beam tube is a very promising aspect since it allows the determination of the cavity phase shift and the second-order Doppler shift. An efficient pulsed operation is possible with a sacrifice in stability of about one to two orders of magnitude. If flicker noise should be a limiting factor, it can be circumvented by simultaneous beam velocity modulation, i. e., by additionally stepping the pulse frequency. This reduces the low frequency noise. Thus, cavity phase shift measurements with a precision equal to the best stabilities of the beam tubes on which the system is used appear quite feasible. First tentative experiments using NBS-5 have been performed; the results are reported elsewhere[7].

The application of the measured velocity distribution to the use of microwave power shift results in accuracy evaluations of cesium beam tubes is quite feasible. Experimental results have been obtained[7] with NBS-5 which demonstrate already an evaluated accuracy of 2×10^{-13} using the power shift method.

Furthermore, not only can the second-order Doppler effect be evaluated but an experimental check of the second-order Doppler equation itself appears feasible, since the second-order Doppler shift is quadratic in v as compared to the linear dependence on v of the phase shift. We note, however, that such a check by another method has already been made[8]. Because the cavity phase shift is recognized as the most severe accuracy limitation to all cesium beam devices, the pulse method may have importance in the accuracy evaluation of most cesium beam standards. Its usefulness may go beyond applications in primary standards laboratories because the pulse method can be applied to almost any existing cesium standard. Thus, commercial standards, such as time scale members, can be evaluated with respect to absolute accuracy, and can periodically be checked. This aspect might have importance for international time scale generation and coordination. The check which this method allows on the velocity distribution, which is largely determined by the beam optics, gives it the potential of being a quantitative test of beam tube alignment.

Acknowledgements

The authors thank J. A. Barnes for his assistance and encouragement in all phases of this work, W. D. McCaa and D. A. Howe for assistance in some phases of this work, A. S. Risley for making available the microwave sweep system, and Patsy J. Tomingas for efficient manuscript preparation.

References

1. G. Becker, B. Fischer, G. Kramer, E. K. Muller, PTB Mitteilungen 79, 77 (1969).

2. A. G. Mungall, Metrologia 8, 28 (1972).

3. D. J. Glaze, IEEE Trans. on Instr. and Meas. IM-19, 156 (1970).

4. H. Hellwig, J. A. Barnes, D. J. Glaze, P. Kartaschoff, U. S. Nat. Bur. Stand. Technical Note 612 (1972).

5. H. Hellwig, J. A. Barnes, D. J. Glaze, Proc. 25th Annual Symposium on Frequency Control, Fort Monmouth, N. J., 309 (1971).

6. N. F. Ramsey, Molecular Beams. Oxford: University Press, 1956.

7. D. J. Glaze, H. Hellwig, Stephen Jarvis, Jr., David W. Allan, A. E. Wainwright, Proc. 27th Annual Symposium on Frequency Control, Fort Monmouth, N. J., (1973).

8. H. E. Ives, G. R. Stillwell, J. Opt. Soc. Am 28, 215 (1938).

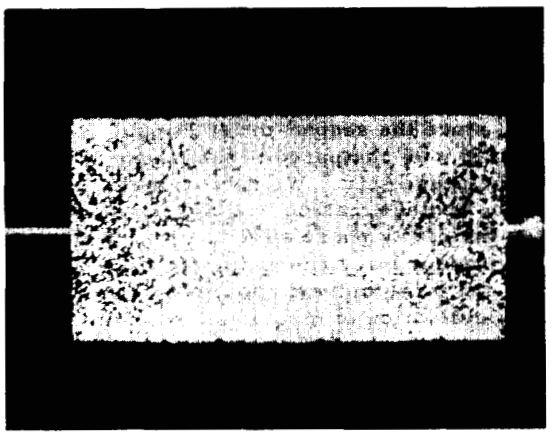

Fig. 1.

Microwave pulse (approx 5 μs) sampled at X-band. Horizontal scale 0.5 μs/division.

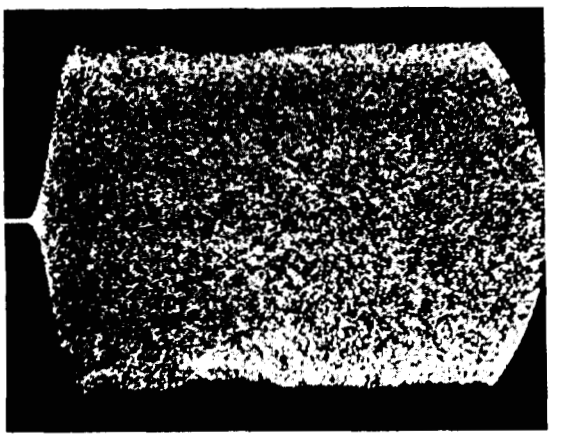

Fig. 2.

Leading edge of the microwave pulse sampled at X-band. Horizontal scale: 2 ns/division.

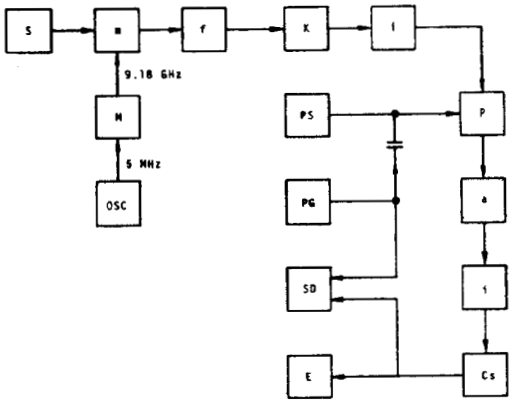

Fig. 3. Block diagram of the measurement system. S = frequency synthesizer, Osc = crystal oscillator, M = frequency multiplier (x 1836), m = mixer, f = filter, K = klystron, i = isolator, p = pin-diode switch, a = attenuator, Cs = cesium beam tube, PS = power supply (pin-diode bias), PG = pulse generator, SD = synchronous detector, E = electrometer.

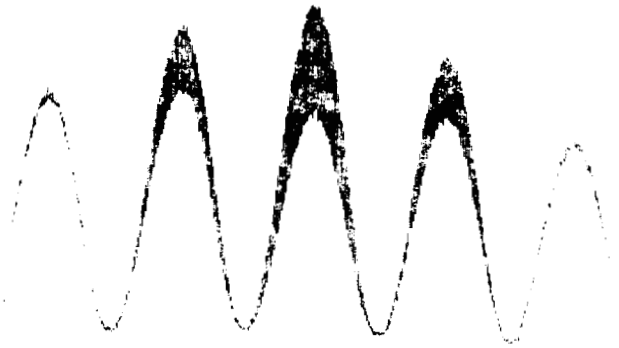

Fig. 5. Spectrum of the beam tube under pulsed operation: T = 1.8 ms, τ_p = 45 μs. The vertical scale is arbitrary. Other recording data are the same as in Fig. 4.

Fig. 6. Spectrum of the beam tube under pulsed operation: T = 1.8 ms, τ_p = 15 μs. Other recording data are the same as in Fig. 4. The short pulses do not allow resolution of the different transitions at the given magnetic field setting.

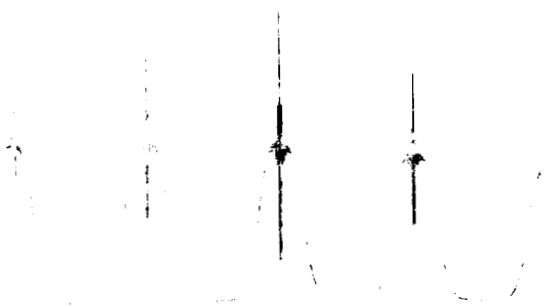

Fig. 4. Spectrum of the beam tube under normal cw operation. The separation between the main peaks is about 40 kHz. The sweep speed was 50 Hz/s. The recording time constant was 0.1 s. The vertical scale is arbitrary.

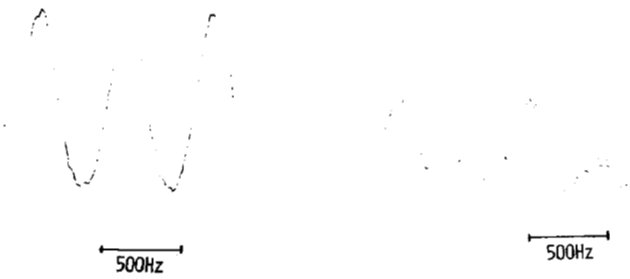

Fig. 7 and 8.

Pulsed operation of the beam tube. High resolution recording of the Ramsey pattern at the peak of the magnetic field independent transition. The frequency scale is indicated, the recording time constant was 1 s. Fig. 7. T = 1.8 ms, τ_p = 15 μs; Fig. 8: T = 1.2 ms, τ_p = 15 μs. The Ramsey period for the fundamental velocity is given by 1/T for both figures. In Fig. 8 the first sub-harmonic velocity corresponding to a period of 1/2T is also contributing.

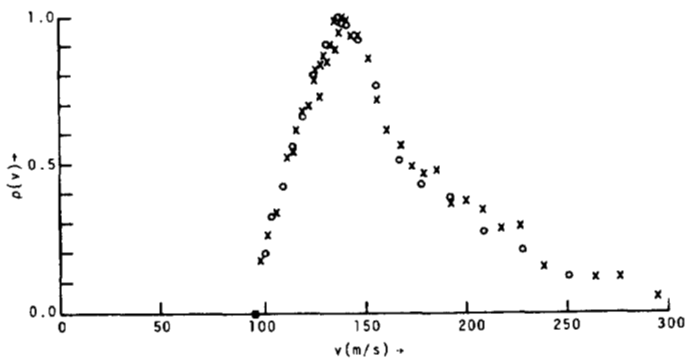

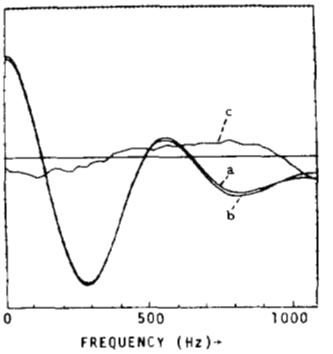

Fig. 9. Velocity distribution of the beam tube. Crosses are obtained with τ_p = 45 μs, circles with τ_p = 15 μs. The distribution function is normalized to 1.0 at the peak.

Fig. 10. Comparison of the experimentally measured Ramsey pattern under normal, cw operation (a) with a pattern (b) which was numerically calculated from Fig. 9. Zero on the frequency scale is the center of the Ramsey pattern. Also depicted is the difference (c) between these two curves using a magnification factor of 4.

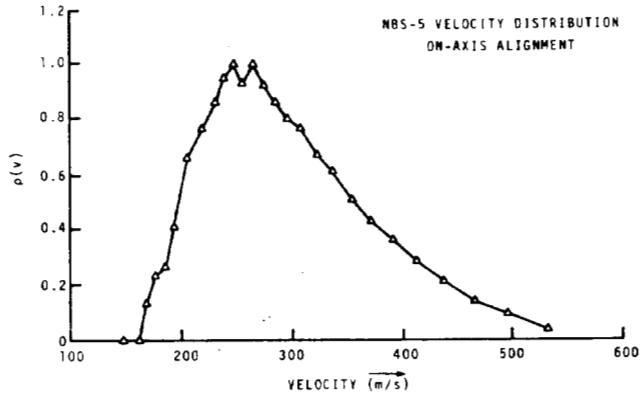

Fig. 11.

Velocity distribution of NBS-5. Long pulse method. The distribution function is normalized to 1.0 at the peak.

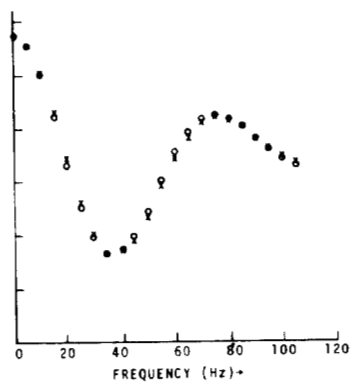

Fig. 12.

Comparison of the experimentally measured Ramsey pattern of NBS-5 under normal cw operation (crosses) with a pattern which was numerically calculated from Fig. 13. Zero on the frequency scale is the center of the Ramsey pattern.

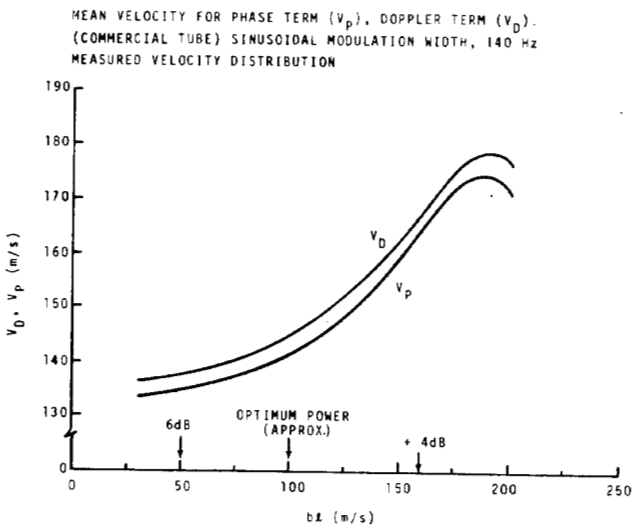

Fig. 13. Effective velocities v_D and v_P as a function of microwave power. Commercial tube, calculated from distribution of Fig. 11.

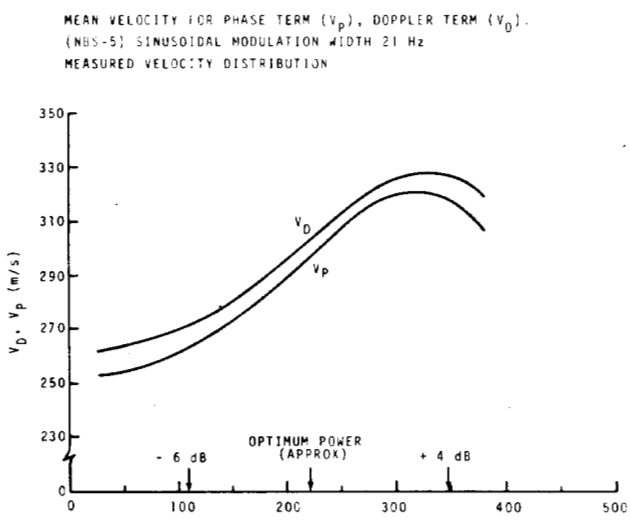

Fig. 14 Effective velocities v_D and v_P as a function of microwave power, NBS-5. Calculated from distribution of Fig. 11.

Fig. 15, 16 & 17 Effective velocity v_p as a function of sinusoidal modulation deviation for three different velocity distributions. Parameter: microwave power. Optimum modulation width corresponds to deviation of one half linewidth.

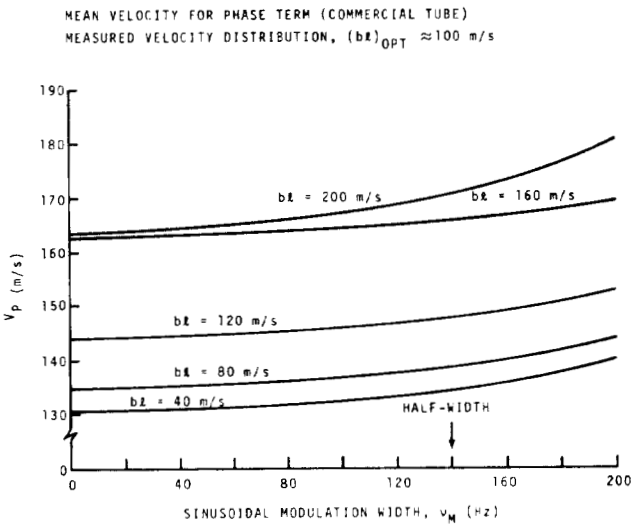

Fig. 15: Commercial tube (distribution Fig. 9).

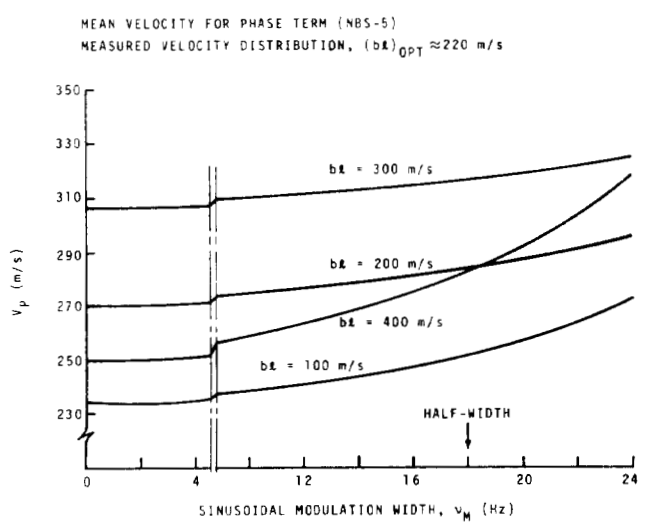

Fig. 16: NBS-5, off-axis alignment (distribution of Fig. 11 in Ref. [7]).

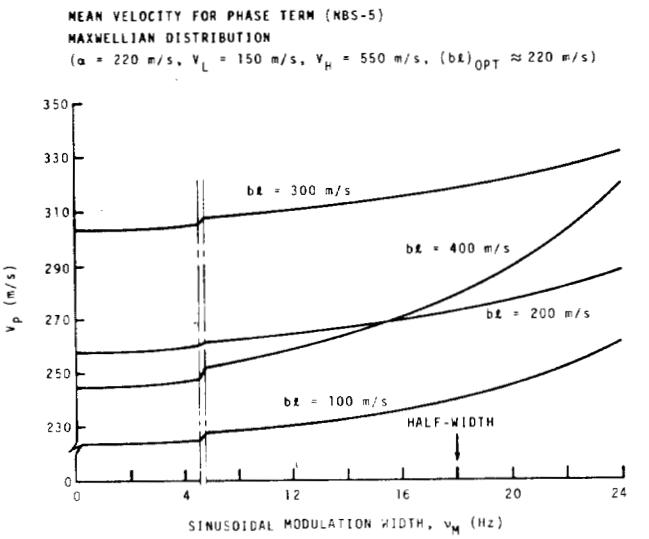

Fig. 17: Maxwellian distribution, matched to NBS-5.